

LASER APPLICATIONS

https://doi.org/10.1070/QEL16507

Defectoscopy of $ZnGeP_2$ single crystals using a strontium vapour laser

A.I. Gribenyukov, S.N. Podzyvalov, A.N. Soldatov,
A.S. Shumeiko, N.A. Yudin, N.N. Yudin, V.Yu. Yurin

Abstract. **A modified method of optical defectoscopy of $ZnGeP_2$ single crystal plates using a strontium vapour laser (λ = 1.03 and 1.09 μm) is proposed based on shadow imaging of internal defects in plates cut parallel to the (100) plane. It is shown that the use of a strontium vapour laser with a wavelength of 6.45 μm makes it possible to study inhomogeneities in large-size $ZnGeP_2$ samples. The possibility of fabricating a projection defectoscope for monitoring breakdown development in $ZnGeP_2$ crystals is considered.**

Keywords: *self-contained lasers, defectoscope, single crystal.*

To date, compact high-power tunable solid-state sources emitting in the range of 3–5 μm are developed and produced commercially in Russia, China, and the USA. As is known, mid-IR lasers can be used in missile defence systems, medicine, gas analysis, and spectroscopy [1–4]. As pump sources for broadband or broadly tunable optical parametric oscillators based on $ZnGeP_2$ crystals, one uses pulsed lasers emitting at wavelengths near ~2 μm [5, 6]. $ZnGeP_2$ single crystals can be also widely used as nonlinear optical crystals to obtain terahertz laser radiation by difference frequency generation from two mid-IR lasers [7–11]. Among a variety of nonlinear optical crystals, the $ZnGeP_2$ single crystal is most appropriate for solving these problems owing to the unique combination of its characteristics, such as a broad transparency range (1–12 μm); high nonlinear-optical quality factor $M = 112\times10^{-24}$ m^2 V^{-2} [$M = d^2/n_p n_i n_s$, where $d = 2\chi^{(2)}$ is the second-order nonlinear polarisability coefficient and $n_{p,i,s}$ are the refractive indices for the pump, idler, and signal waves, respectively]; and a high breakdown threshold, which, at a pulse duration of ~10 ns, reaches about 50 MW cm^{-2} at λ = 2.09 μm and 150 MW cm^{-2} at λ = 2.96 μm [12].

The main problem with using complex crystals is related to the existence of local variations in their composition, i.e., inhomogeneities of up to macroscopic sizes (1–50 μm), whose refractive index and absorption coefficient differ from the corresponding values of the matrix [13]. It is clear that the possibility of developing practical devices with nonlinear optical elements made of $ZnGeP_2$ single crystals depend on the reproducibility of their properties and, hence, requires the development of not only technological control methods but also of the methods of defect detection and identification at all the stages of the technological chain. The control of the size and geometry of defects, as well as of their position in the crystals, plays an important role in cutting the crystals into working elements and may help to select the methods of post-growth treatment of crystals needed to modify their properties. It is clear that control methods should be fast, contactless, and nondistractive. Optical defectoscopy is most appropriate for solving this problem. Since the $ZnGeP_2$ crystal transparency window lies in the IR spectral region (this crystal in nontransparent in the visible region), internal defects appearing in the process of production of nonlinear elements for different applications must be detected and visualised using IR radiation.

In this work, we study defects in $ZnGeP_2$ single crystals by recording and analysing IR images obtained in a transmission mode. The IR images were formed using a strontium vapour laser and analysed using a BeamCube (Ophir) laser beam analyser.

Strontium vapour lasers emit in the IR region at eight transitions with wavelengths of ~1.03, 1.09, 2.6, 3.06, 2.69, 3.01, 2.92, and 6.45 μm [14]. All the listed laser lines lie in the transparency region of the $ZnGeP_2$ single crystal (Fig. 1).

The transmission of $ZnGeP_2$ single-crystal plates was measured according to the scheme shown in Fig. 2. The absorption coefficients with allowance for multiple reflections from the plane-parallel planes of the plates were calculated by the formulas

$$\alpha^{e,o} = -\frac{1}{d}\ln\{\sqrt{[A^2 + (R^{e,o})^{-2}]} - A\}, \quad (1)$$

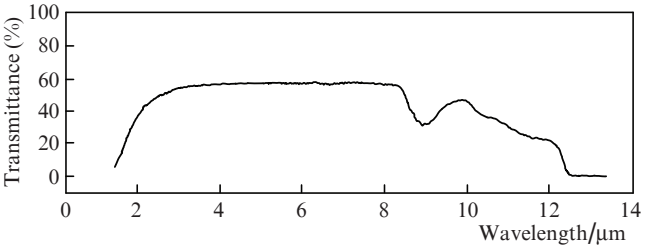

Figure 1. $ZnGeP_2$ plate transmission spectrum measured with an FT-801 Fourier-transform spectrophotometer (Simex).

A.I. Gribenyukov Institute of Monitoring of Climatic and Ecological Systems, Siberian Branch, Russian Academy of Sciences, prosp. Akademicheskii 10/3, 634055 Tomsk, Russia; National Research Tomsk State University, prosp. Lenina 36, 634050 Tomsk, Russia; **S.N. Podzyvalov, A.N. Soldatov, A.S. Shumeiko, N.A. Yudin, N.N. Yudin, V.Yu. Yurin** National Research Tomsk State University, prosp. Lenina 36, 634050 Tomsk, Russia; e-mail: yudin@tic.tsu.ru

Received 30 August 2017; revision received 5 February 2018
Kvantovaya Elektronika **48** (5) 491–494 (2018)
Translated by M.N. Basieva

$$R^{e,o} = \frac{(n^{e,o}-1)^2}{(n^{e,o}+1)^2}, \quad (2)$$

$$T^{e,o} = \frac{I^{e,o}}{I_0} = \frac{(1-R^{e,o})^2 \exp(-\alpha^{e,o} d)}{(1-R^{e,o})^2 \exp(-2\alpha^{e,o} d)}, \quad (3)$$

$$T = \frac{1}{I_0} = \frac{T^o}{2}[1+\cos^2\theta] + \frac{T^e}{2}\sin^2\theta, \quad (4)$$

where $\alpha^{e,o}$ are the absorption coefficients for extraordinary and ordinary waves, respectively; d is the plate thickness; $R^{e,o}$ are the reflectivities; $n^{e,o}$ are the refractive indices; $T^{e,o}$ are the transmittances for the corresponding waves; θ is the angle between the radiation direction (wave vector) an the optical axis of the crystal; $I^{e,o}$ are the intensities of extraordinary and ordinary waves; I and I_o are the intensities of radiation passed through the crystal and incident on it; T is the sample transmittance; and $A = (1 - R^{e,o})^2/[2T(R^{e,o})^2]$.

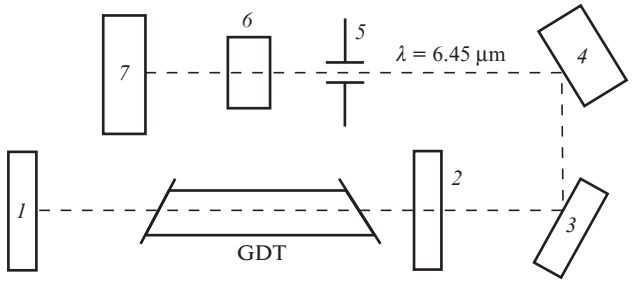

Figure 2. Experimental scheme for measuring transmission of $ZnGeP_2$ single crystal at wavelengths of 6.45, 1.03, and 1.09 μm: (*1*, *2*) cavity mirrors with gas-discharge tube (GDT) of a strontium vapour laser between them; (*3*) deflecting aluminium mirror; (*4*) diffraction grating; (*5*) aperture; (*6*) studied $ZnGeP_2$ single crystal plate; (*7*) power meter (Ophir).

To solve system (1)–(4), which has only three independent equations but four indeterminates, one needs an additional relation. This can be the ratio of absorption coefficients of the waves with extraordinary and ordinary polarisations. The spectral dependence of this ratio,

$$K = \frac{\alpha^e}{\alpha^o} = 1.08 + 1.83\exp\left[\frac{-(\lambda-2.26)^2}{0.29}\right] \quad (5)$$

was found by Gaussian approximation of the experimental data obtained for oriented $ZnGeP_2$ crystals grown at the Institute of Monitoring of Climatic and Ecological Systems, Siberian Branch, Russian Academy of Sciences. The measurements were performed independently at three organisations, namely, IMCES SB RAN; INRAD, Inc. (USA); and Cleveland Crystals, Inc. (USA). Even the first measurements showed that the $ZnGeP_2$ single-crystal plates 6 mm thick transmit radiation of strontium lasers at a wavelength of 6.45 μm (laser beam diameter 12.5 mm, average power 485 mW) almost without absorption, i.e., with $T \approx 55\%$, which corresponds to the absorption coefficient $\alpha_{6.45} \approx 0.08$ cm^{-1}. The transmittance at wavelengths of 1.03 and 1.06 μm was ~1%, which corresponds to absorption coefficient $\alpha_{1.03} \sim 6.3$ cm^{-1}.

Complex crystals always have local variations in their composition, i.e., inhomogeneities of up to macroscopic size (1–50 μm) with refractive indices and absorption coefficients different from the average values of these parameters for the crystal itself [13].

Thus, radiation with a wavelength of ~1 μm allows detection of defects with sizes of ~0.5 μm, but, in thick samples, defects cannot be seen due to high absorption losses. The minimum sizes of objects detectable by radiation with a wavelength of 6.45 μm are restricted to ~3 μm by the detecting radiation wavelength. Nevertheless, measurements at this wavelength are of great interest due to a low absorption by the material and the minimum scattering effect, since the scattering efficiency is proportional to the parameter $(a/\lambda)^n$, whose exponent n may change from unity (at inhomogeneity size $a \approx \lambda$) to four (at $a \ll \lambda$). Correspondingly, the shadow image of defects at wavelength $\lambda = 6.45$ μm should have higher contrast and resolution and, in addition, this wavelength allows defectoscopy in thick samples. Of course, we must take into account that, to visualise defects at a wavelength of 6.45 μm, it is necessary to use detectors sensitive in this wavelength region, for example, thermal imagers. Thus, due to the unique combination of operation wavelengths, strontium lasers can be used for detecting large (exceeding 3 μm) defects in samples measuring 10–15 cm, while detection of defects with sizes of ~1 μm requires special preparation of plates with a thickness of ~5 mm.

In the present work, we detected internal defects in $ZnGeP_2$ single crystals by visualisation of shadow IR images obtained due to propagation of strontium laser radiation with wavelengths of 1.03 and 1.09 μm through the single crystal as was done in [15]. The choice of these laser wavelengths is explained by wide availability of detectors operating within a wavelength range up to 1.1 m.

Defects in a $ZnGeP_2$ single crystal plate with dimensions of 23×17×6 mm were visualised according to the scheme shown in Fig. 3. We used a strontium vapour laser with a BeO ceramics discharge tube 2.6 cm in diameter and 80 cm long. The unstable telescopic cavity was formed by a spherical highly reflecting aluminium mirror (*1*) with a curvature radius of 300 mm and an output spherical convex mirror (*2*) with a curvature radius of 10 mm and a virtual focus, which formed a plane-parallel laser beam. The average power of the strontium vapour laser (after an IKS-1 filter) was ~500 mW at wavelengths of 1.03 and 1.09 μm.

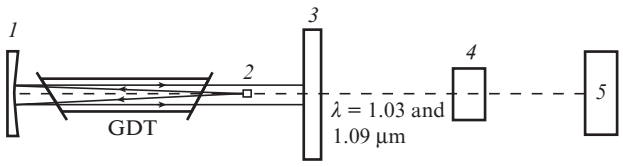

Figure 3. Experimental scheme for defectoscopy of $ZnGeP_2$ single crystals: (*1*, *2*) cavity mirrors; (*3*) IKS-1 optical filter; (*4*) $ZnGeP_2$ single crystal plate; (*5*) BeamCube beam analyser (Ophir).

Examples of shadow images of internal defects obtained using a BeamCube laser beam analyser are shown in Figs 4 and 5. Figure 4 presents the shadow image of a part of a crack inside a $ZnGeP_2$ single crystal plate, which is unseen visually. Figure 5 presents the total image of the internal crack. This image is formed by gluing the images obtained by shifting the detector matrix for a distance equal to its length. As a result, we have the image of the entire studied area with complete information on the internal defects of the crystal.

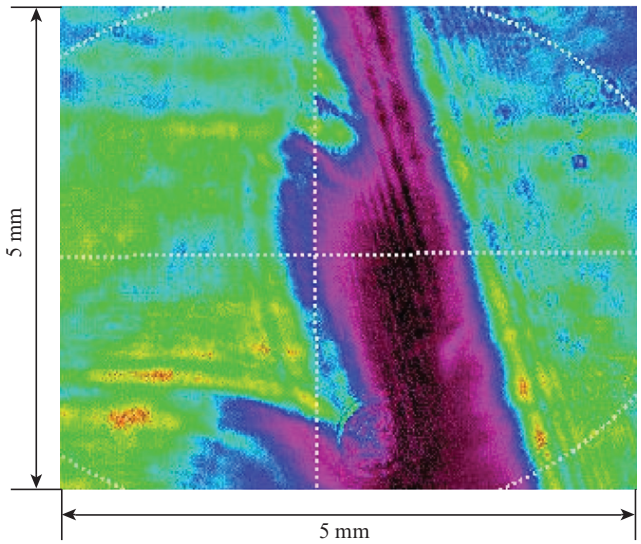

Figure 4. Shadow image of a part of an internal defect in a $ZnGeP_2$ plate obtained using a strontium vapour laser emitting at wavelengths of 1.03 and 1.09 μm.

A drawback of the proposed method is that the dimensions of detected defects are limited by the detector pixel size. To increase the method sensitivity and have the possibility of using low-cost detector matrices, we propose to upgrade this method and create a laser projection defectoscope based on a master-oscillator–amplifier system shown in Fig. 6.

The principle of operation of this projection defectoscope is as follows: a master-oscillator (GDT1) beam propagates through a narrowband optical filter (*3*), which separates radiation with a required wavelength, and then is focused by lens *5* into the studied region of the single crystal. Since the refractive index of the $ZnGeP_2$ single crystal in the near- and mid-IR regions is ~3 [16], the laser beam in the single crystal almost does not diverge. The radiation passed through the crystal falls on lens *7*, which forms a plane-parallel beam carrying information on the internal defects of the single crystal. This beam passes through GDT2, is amplified, and falls on lens *8*, which magnifies the image and projects it on the screen (*9*). To visualise defects in single crystals at wavelength λ =6.45 μm according to the scheme shown in Fig. 6, we suggest to use a thermal imager (*10*), which records the temperature distribution pattern from the screen. This projection defectoscope may also serve to visualise defects using radiation with wavelengths of 1 and 3 μm, for which the screen should be replaced by a detector operating in this spectral range. One

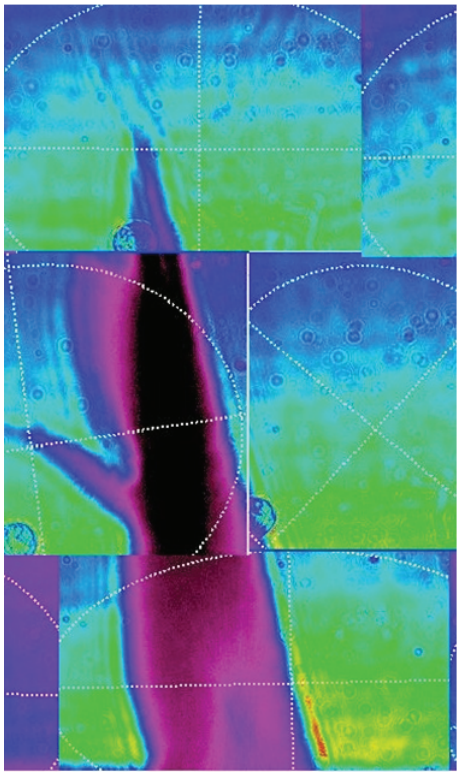

Figure 5. Glued image of a defect with linear dimensions exceeding the dimensions of the analyser matrix.

can scan the image plane with a photodetector and then glue the obtained images. The minimum linear dimensions of detected defects are limited by the recording wavelength to 0.5–3 μm (depending on the wavelength). This visualisation method can find application for recording fast processes occurring inside single crystals, for example, at the instant of optical breakdown or during a pre-breakdown state, owing to the ability of strontium vapour lasers to operate with high pulse repetition rates (~1 MHz) [17]. To record such processes, it is necessary to synchronise the pulsed pump laser with the detector (as was done in [18]).

Thus, our investigations confirm that IR strontium vapour lasers are promising for defectoscopy of $ZnGeP_2$ single crystals by a shadow method. It is noted that it is possible to create a projection defectoscope with a minimum resolution of ~0.5 μm and a frame repetition rate of ~1 MHz for monitoring breakdown development in $ZnGeP_2$ single crystals.

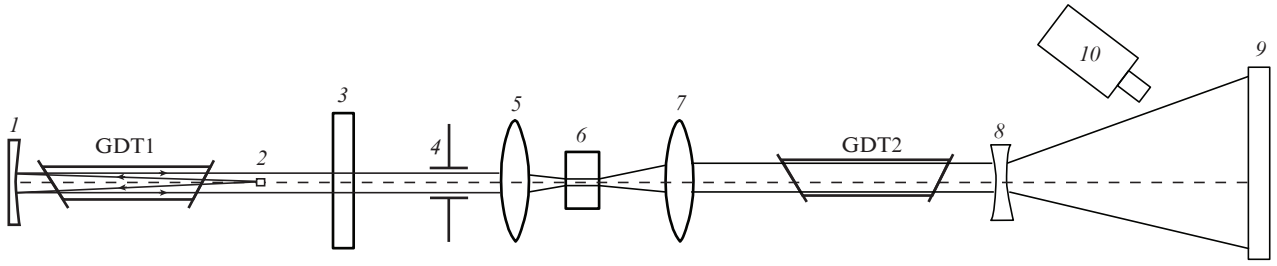

Figure 6. Laser projection defectoscope scheme: (*1*, *2*) cavity mirrors; (GDT1, GDT2) gas discharge tubes of strontium vapour lasers (master oscillator and amplifier, respectively); (*3*) narrowband optical filter; (4) aperture; (*5*, *7*, *8*) lenses; (*6*) studied $ZnGeP_2$ single crystal; (*9*) screen; (*10*) camera (thermal imager).

References

1. Godard A., Lefebvere M., Hassani S., Galter P. *Technol Opt. Countermeas. IV*, **6738**, 67380C-1 (2007).
2. Lippert E., Nicolas S., Arisholm G., Stenersen K., Rustad G. *Appl. Opt*., **45** (16), 3839 (2006).
3. Stoeppler G., Thilmann N., Pasiskevicius V., Zukauskas A., Canalias C., Eichhorn M. *Opt. Soc. Am*., **20** (4), 4509 (2012).
4. Bochkovskii D.A., Vasil'eva A.V., Matvienko G.G., Polunin Yu.P., Romanovskii O.A., Soldatov A.N., Kharchenko O.V., Yudin N.A., Yakovlev S.V. *Opt. Atmosf. Okeana*, **24** (11), 985 (2011).
5. Zakharov N.G., Antipov O.L., Sharkov V.V., Savikin A.P. *Quantum Electron*., **40** (2), 98 (2010) [*Kvantovaya Elektron*., **40** (2), 98 (2010)].
6. Zhou Ren-Lai, Ju You-Lun, Wang Wei, Zhu Guo-Li, Wang Yue-Zhu. *Chin. Phys. Lett*., **28** (7), 074210 (2011).
7. Shi W., Ding Y.J. *Appl. Phys. Lett*., **83**, 848 (2003).
8. Tanabe T., Suto K., Nishizawa J., Sasaki T. *J. Phys. D: Appl. Phys*., **37**, 155 (2004).
9. Luo C., Reimann K., Woerner M., Elsaesser T. *Appl. Phys*., **78**, 435 (2004).
10. Shi W., Ding Y.J. *Appl. Phys. Lett*., **84**, 1635 (2004).
11. Shi W., Ding Y.J., Schunemann P.G. *Opt. Commun*., **233**, 183 (2004).
12. Andreev Yu.M., Voevodin V.G., Geiko P.P., Gorobuts V.A., Lanskaya O.G., Petukhov V.O., Soldatkin N.P., Tikhomirov A.A. *Lidarnye sistemy i ikh optiko-elektronnye elementy* (Lidar Systems and Their Electrooptical Elements) (Tomsk: Institute of Atmospheric Optics SB RAN, 2004).
13. Libenson M.N., Yakovlev E.B., Shandybina G.D. *Vzaimodeistvie lasernogo izlucheniya s veshchestvom (silovaya optika). Konspekt lektsii. Chast' I. Pogloshchenie lazernogo izlucheniya v veshchestve* (Interaction of Laser Radiation with Matter (Power Optics). Notes of lectures. Part I. Absorption of Laser Radiation in Matter) Ed. by V.P. Veiko (St. Petersburg: ITMO, 2008).
14. Soldatov A.N., Latush E.L., Chebotarev G.D., Yudin N.A., Vasil'eva A.V., Polunin Yu.P., Prutsakov O.O. *Impul'sno-periodicheskie lasery na parakh strontsiya i kal'tsiya* (Repetitively Pulsed Strontium and Calcium Vapour Lasers (Tomsk: TML-Press, 2012).
15. Demin V.V., Polovtsev I.G., Kamenev D.V. *Izv. Vyssh. Uchebn. Zaved., Ser. Fiz*., **58** (10), 106 (2015).
16. Boyd G.D., Buehler E., Storz F.G. *Appl. Phys. Lett*., **18** (7), 301 (1971).
17. Soldatov A.N., Yudin N.A., Vasil'eva A.V., Kolmakov E.A., Polunin Yu.P., Kostyrya I.D. *Quantum Electron*., **42** (1), 31 (2012) [*Kvantovaya Elektron*., **42** (1), 31 (2012)].
18. Evtushenko G.S., Trigub M.V., Gubarev F.A., Torgaev S.N. *Izv. Tomsk. Polytekh. Univ.*, **319** (4), 154 (2011).